Fracture Properties of Geopolymer Concrete Based on Metakaolin, Fly Ash and Rice Rusk Ash

Eliane Fernandes Côrtes Pires[a], Claúdio Mesquita Campinho de Azevedo[a], André Rocha Pimenta[b],

Felipe José da Silva[a,b]*, Fathi Aref Ibrahim Darwish[a]

[a]Departamento de Engenharia Civil, Universidade Federal Fluminense, Niterói, RJ, Brasil
[b]Curso Técnico em Mecânica Industrial, Instituto Federal do Rio de Janeiro, Paracambi, RJ, Brasil

Geopolymers are exclusively mineral nature and are considered an alternative to materials based on Portland clinker, whose production accounts for about 5% of anthropogenic CO_2 emissions in the world. The geopolymer cement concrete (GCC) may be prepared from natural oxide-aluminosilicates such as metakaolin (MK), or synthetic, such as fly ash (FA) together with active silica contained in the rice husk ash (RHA). The fracture properties of the Portland cement concrete (PCC) with 25 MPa and 50 MPa, and of three different geopolymeric concretes with the same strength Classes were determined for comparative analysis. The aim of this study is to provide support to begin the use of geopolymers in the reinforced concrete precasting Industry. Three-point bending tests of notched beams with a/d (notch depth/beam depth) of 0.5 from RILEM TC80-FMT Recommendations were used to determine the critical values of K, G, R and J-integral for crack propagation under mode I. The results showed that the geopolymeric concretes exhibit similar mechanical behavior and fracture properties higher that those determined in PCC for the same strength class.

Keywords: *geopolymer, concrete, fracture toughness, fly ash, rice husk ash.*

1. Introduction

The geopolymers are considered ceramic materials. The ionic-covalent nature of their molecular bonds, the extent of the chains and the structural arrangement they form lead to particular properties in the fresh and hardened states[1,2,3]. Although the geopolymer slurry shows less autogenous retraction than Portland cement paste, during geopolymerization the reaction medium requires water as the ionic conduction vehicle[4]. This water is essential to maintain the degree of saturation necessary for the geopolymerization to reach the required degree[5,6]. Excess water, as well as scarcity in the mixture, causes disequilibrium in the reaction and leads to unstable structure or with numerous physical discontinuities[7]. Despite the control, in practice it is extremely difficult to prevent discontinuities to be formed during geopolymerization since residual elastic tensions tend to be alleviated with the formation of discontinuities, often with the creation of microcracks[8].

The mechanical behavior of mortars and geopolymer concrete revealed that they are like rocks and concretes of Portland cement, that is, they are classified as "quasi-brittle". This category refers to the fact that they present the elastic-plastic localized deformation phenomenon in the region immediately ahead and around the end (tip) of preexisting discontinuities when submitted to mechanical stresses. In the case of discontinuities of acute elliptic geometry, as

occurs with cracks, the stress concentration makes it easy to reach the limit of tensile strength of the material leading to rupture, sometimes catastrophic[9]

The so-called Linear Elastic Fracture Mechanics (LEFM) and its derivation for the Nonlinear Fracture Mechanics (NLFM) are sciences that study the influence of the presence of these sharp discontinuities inside the material under mechanical loading. Different models have emerged over the last three decades to quantify the fracture toughness of *quasi*-brittle materials by considering the effects of the region of localized elastoplastic deformation (*Fracture Process Zone*, FPZ). However, most models require the separation of elastic and plastic components of the FPZ, which could only occur in controlled situations of successive loading and unloading in a piece of suitable geometry sensitized by a notch in a certain section, more loaded.

The 3-point bending test with concentrated load in the middle of the span became a standard test for *quasi*-brittle materials, whereas, for metals, the compact tensile test remained the most used. The pioneering works of Hillerborg[10], Jenq & Shah[11] and Bazant & Kazemi[12] provided as early as the 90s technical recommendations by RILEM[13]. The test model proposed by RILEM Technical Committee 80 - Fracture Mechanics Tests (TC-80 FMT) became a reference standard, as an alternative to ASTM C 1018, which defined the tougness indixes under simple bending of non-notched beams with applied load in the center of the span. The main criticism associated with this model is due to the fact it is based

on readings of maximum deflections at critical moments, such as the formation of the 1st crack which is difficult to determine. As there is no macroscopic stress concentrator to aid in the localized formation of the FPZ, the crack can form in any position near the loaded section, which compromises the characterization by preventing any correlation between the size of the defect and the load applied in the material[9].

Some fracture parameters such as the elastic energy release rate, (G), stress intensity factor (K), J-integral, fracture resistance ® were adopted to characterize concretes of Portland cement and geopolymer.

The fracture toughness was used as a measure of the resistance of the material to the crack propagation[14]. The stress intensity factor was proposed in 1957 by Irwin to describe the intensity of the elastic behavior of the crack tip and symbolizes the linear elastic fracture mechanics. These parameters are presented below, but only for definition. More details could be obtained from LEFM Compendiums[15-17].

The critical stress intensity factor in the mode I of crack opening, called K_{Ic}, is determined when $a = a_c$, by[18]:

$$\%m/mCu = \frac{m_{Cu}}{m_{Cu} + m_{Sn}} \times 100\% \quad (1)$$

where P is the active load, a is the notch extension and equal to 50 mm, b is the width of the small beam and equal to 100 mm, d is the height of the notch equal to 100 mm, $F_3 (a/d)$ is a function given by:

$$\%m/mSn = \frac{m_{Sn}}{m_{Cu} + m_{Sn}} \times 100\% \quad (2)$$

The critical rate of strain energy release for propagation of a crack extension unit was obtained by:

$$d_p = \frac{k\lambda}{\beta \cos\theta} s \quad (3)$$

where K_{Ic} is the stress intensity factor in the critical state and E is the modulus of elasticity calculated by the following[13]:

$$C_{DCE} = (CPE)^{\frac{1}{N}} \times R_{Ic}^{\left(\frac{1}{N}-1\right)} \quad (4)$$

where S is the span, equal to 400 mm, d is the height of the beam, equal to 100 mm and b is the width of the beam, equal to 100 mm. The parameter $V_1(\alpha_0)$ was calculated from the following equation[13]:

$$V_1(\alpha_0) = 0,76 - 2,28\alpha_0 + 3,876\alpha_0^2 - 2,04\alpha_0^3 + \frac{0,66}{(1-\alpha_0)^2} \quad (5)$$

where: $\alpha_0 = \frac{a_0}{d} = \frac{50}{100} = 0.5$

The initial compliance, or initial flexibility, was calculated by the following:

$$C_i = \frac{CMOD_i}{P_I} \quad (6)$$

where the $CMOD_i$ is provided by the clip gauge, in a load acting on the elastic phase, P_i.

R-curve studies stable crack growth and response to the effects of increased toughness.

Obtaining curves R_I (resistance to fracture) was proposed by Ouyang & Shah[19] from K_{Ic} and $CTOD_c$ and expressed by:

$$R = \beta\psi(a - a_0)^{d_2} \quad (7)$$

where a_0 is the initial notch length of 50 mm; The coefficients α (equation 8) and β (equation 9) are determined from the biparametric model of fracture:

$$\alpha = \mu + \sqrt{\mu^2 + 1} \quad (8)$$

$$\beta = \frac{(K_{Ic})^2 (d_1\alpha - \alpha + 1)}{E\alpha(d_1 - d_2)(\alpha a_{0d} - a_0)^{d_2}} \quad (9)$$

The coefficient μ is calculated as follows:

$$\mu = \frac{\pi E^2 f_1^2 CTOD_c}{32 a_0 (K_{Ic})^2 f_2^2} \quad (10)$$

where E is the tangent modulus of elasticity, f_1 and f_2 are equal to 1.123 and 1.420, respectively, tabulated for notched beam in the center of the span, under 3-point bending and with span/height ratio equal to 4.

The roots of the equation, d_1 and d_2, are given by equation 11:

$$d_1, d_2 = \frac{1}{2} + \frac{\alpha - 1}{\alpha} \pm \left[\frac{1}{4} + \frac{\alpha - 1}{\alpha} - \left(\frac{\alpha - 1}{\alpha}\right)^2\right]^{\frac{1}{2}} \quad (11)$$

So,

$$\psi = 1 - \frac{d_2\alpha - \alpha + 1}{d_1\alpha - \alpha + 1}\left(\frac{\alpha a_0 - a_0}{a - a_0}\right)^{d_2 - d_1} \quad (12)$$

$$CTOD_c = \frac{6P_c S a_c \sqrt{(1 - \beta_0)^2 + (1,081 - 1,149\alpha_c)(\beta_0 - B_0^2)}}{Ed^2 b} \quad (13)$$

$$\alpha_c = \frac{a_c}{d} \quad (14)$$

$$\beta_0 = \frac{a_0}{a_c} \quad (15)$$

The J-integral was proposed in 1968 by Rice[16] to characterize the intensity of elastic-plastic behavior at the crack tip and symbolizes the mechanics of elastic-plastic fracture.

A J-integral can be determined according to the equation below:

$$J = \frac{2U}{b(d - a_0)} \quad (16)$$

where d represents the width of the specimen and (d - a_0) represents the height of the ligament, a_0 is the crack length

equal to 50 mm, U is the work performed during loading, calculated by integrating the area under the P-δ, (equation 17), where P is the instantaneous load and δ is the displacement of the point of application of the load.

$$U = \int_0^\delta P d\delta \qquad (17)$$

The J_{max} is obtained when $U = U_{max}$, form $P = P_{max}$ and $\delta = \delta_{max}$[16].

This paper presents the fracture parameters of three types of geopolymer (GCC, GCC-20FA, GCC-20FA-RHA), obtained from different raw materials and compared with the results presented by Portland cement concrete (PCC) in two strength classes, 25 MPa and 40 MPa, at 28 days of age.

2. Materials and methods

The fine aggregate was washed river sand with a fineness modulus of 2.66 and maximum dimension, $D_{máx}$, of 24 mm, considered as average size sand. The coarse aggregate used was of gneiss origin with a fineness modulus of 5.72mm, considered as level zero gravel with maximum size of 9.5 mm.

The geopolymer cement used in the manufacturing of the geopolymer concrete beams was provided by Wincret Designer Concrete Products Ltda, based in São Paulo/SP-Brazil. It is commercially called Cement Geo-Pol®, with SiO_2/Al_2O_3 ratio equal to 5.35 and $(Na_2O + K_2O)/SiO_2$ equal to 0.209. The binder is usually supplied in two components, identified by the manufacturer as Component-A: pozzolan-blend and Component B: alkali-polysilicate. For this work, Components A and B were provided separately from the fractions identified as Components A1: metakaolin, A2: unidentified solid-blend, B1: aqueous sodium silicate and B2: potassium hydroxide. The Portland cement used in the reference concrete was the CPIIF-32 manufactured by Lafarge/Mauá S.A. and acquired in the local market. The mass ratio between the constituents of the concrete (of all matrices studied) was 1: 1.26: 0.99 (dry binder: sand: zero gravel) with water/dry binder ratio of 0.36, setting characteristic resistance at 28 days of age, f_{ck}, of 40 MPa. Already for f_{ck} 25 MPa, the mass ratio was 1: 2.00: 1.57 and factor water/dry binder 0.46, according to Table 1.

The potassium hydroxide and sodium silicate solutions were prepared separately and mixed together at the time of molding. The aqueous silicate showed SiO_2/Na_2O ratio of 2.24. The potassium hydroxide solution had 8.7% K_2O. The metakaolin presented a SiO_2/Al_2O_3 ratio of 1.60, specific gravity of 2.52 ± 0.32 kg/dm³, specific surface of 1864.22 m²/kg.

Fly ash (FA) was supplied by the company Pozofly S.A., based in the city of Porto Alegre/RS/Brazil. According to ASTM C618/12a it belongs to class F, of low pozolanicity. Its specific gravity was 2.32 g/cm³ and the specific surface was 312.33 m²/kg. Metakaolin was substituted in 20% volume with fly ash, originating the nomenclature of the GCC-20FA geopolymer matrix. Rice husk ash (RHA) was supplied by TecnoSil S.A., from the Rio Grande do Sul state and originated from biomass burning for steam and energy generation. Its specific gravity was 2.14 kg/dm³, apparent density 890 kg/m³, pozzolanic activity of 625 mg CaO/g. An alternative sodium silicate was made from RHA pre-solubilized to fully replace the commercial sodium silicate. In addition to using 20% FA, this alternative RHA sodium silicate was used resulting in the nomenclature of the GCC-20FA-RHA geopolymer matrix. To determine the fracture properties of plain concrete small beams, 24 notched beams were tested at three loading points, as recommended by RILEM TC80-FMT[13]. Three samples were formed for each matrix (PCC, GCC, GCC-20FA, GCC-20FA-RHA) by grouping each matrix with each strength class (25 and 40 MPa). All specimens were 500 mm x 100 mm x 100 mm, with a span (S) / height (d) ratio of 4, and a notch height (a_0) and beam height (d) ratio of 0.5. The loading rate was 50 ± 15 N/s. The deflection in the middle of the span was monitored through the resistive displacement transducer with electrical course 100 mm, precision of 0.01 mm, mark GEFRAN INC. The crack mouth opening displacement (CMOD) was monitored using clip-gage attached under the beam through the latex rods (Figure 1). All electrical sensors were read using the National Instruments Data Acquisition System Model cDAQ-9217, assisted by the LabView 8.6 software.

3. Results and discussions

P-CMOD curves of both concrete strength class of 25 and 40 MPa are shown in Figures 2 and 3, respectively. In class 25, the geopolymer with the two ashes (GCC-20FA-RHA_25) showed the best results in stiffness, strength and critical value of CMOD.

Table 1. Concrete design parameters of classes 25 and 40 MPa.

Parameters	Class 25	Class 40
Compressive strength characteristic, f_{ck}	25 MPa	40 MPa
Compressive strength of design, f_{cj}	35 MPa	49 MPa
Standard deviation of design,S_d	5.5 MPa	5.5 MPa
Water/Cement ratio,w/c	0.457	0.357
Consumption of binder / m³of concrete	459.52 kg	640.75 kg
Proportion (by mass)	1 : 2.00 : 1.57 : 0.46	1 : 1.26 : 0.99 : 0.36

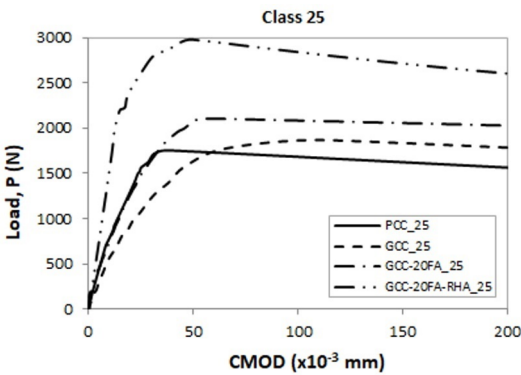**Figure 1.** Clip Gauge placement detail for CMOD reading.

Figure 2. Variation of load with CMOD to 25 MPa strength class of concrete for all matrices studied.
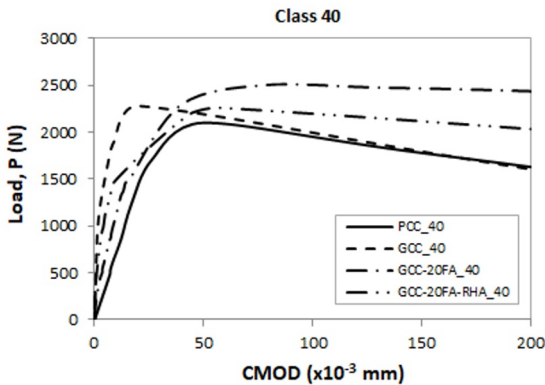

Figure 3. Variation of load with CMOD to 40 MPa strength class of concrete for all matrices studied.

Although less rigid, the standard geopolymer (GCC_25) showed P_{max} and $CMOD_c$ higher than the PCC, indicative of higher toughness. With 20% of FA, stiffness was equivalent, but P_{max} was higher than that of PCC.

In class 40, all geopolymers presented better results than PCC, with emphasis on GCC-20FA_40. In this class, the RHA silicate containing matrix did not repeat the superior performance as in class 25. This could be attributed to the

workability loss of the matrix with the lowest aggregate content even though there was an increase in P_{max}.

Figure 4 shows K_I *versus* Δa for notched beams of the strength class of 25 MPa and the different matrices. The standard geopolymer had a small performance gain in relation to Portland, but the use of FA promoted a greater increase of the stress intensity factor, K_I. As for the influence of the RHA, the use of the sodium silicate of RHA provided a substantial improvement in K_I values of approximately 35% compared to the standard geopolymer.

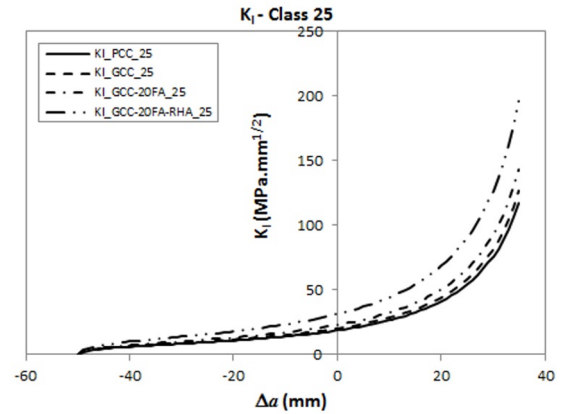A less selective behavior was observed in the beams of the class 40 MPa (Figure 5).

Figure 4. Variation of the stress intensity factor (K_I) with the nominal extension of the crack (Δa) for concrete notched beams of strength class of 25 MPa, with different matrices.

Although the K_I curve of GCC-20FA-RHA_40 has remained above the others, it can be said that all presented
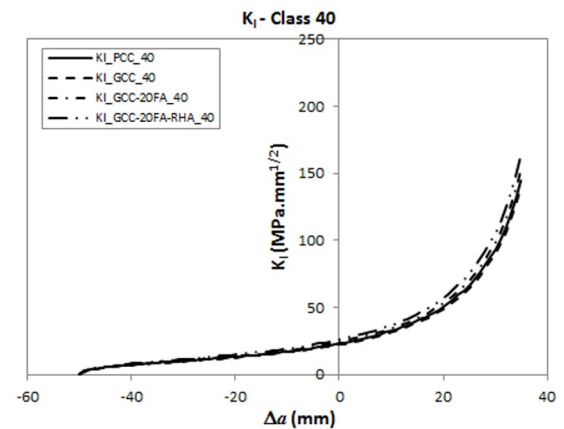

Figure 5. Variation of the stress intensity factor with the extension of the crack for concrete notched beams of strength class of 40 MPa, with different matrices.

similar performance. Another observation is that when compared to the K_I curves of class 25, there was no increase

of toughness with the increase of strength class, except in GCC-20FA-RHA.

Figure 6 shows the G_I values as a function of Δa for beams of class 25 MPa, for the different concrete matrices. As can be seen, the GCC-20FA_25 had the best performance, surpassing the other geopolymers. The emphasis in relation to PCC_25 was almost 100%. In terms of G_I-Δa, the standard geopolymer (GCC_25) and the geopolymer with the two ashes (GCC-20FA-RHA_25) presented similar performances, but both superior to PCC_25 by approximately 60%.
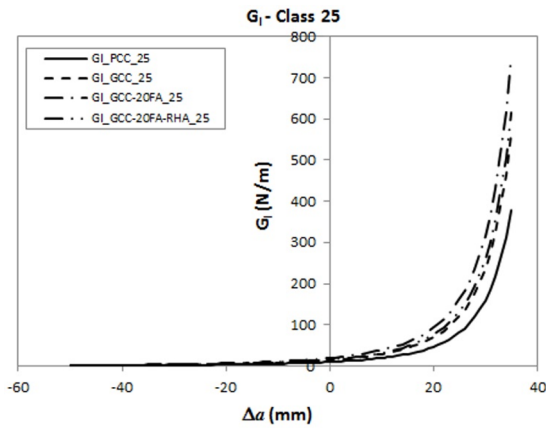
Since G_I is directly proportional to $(K_I)^2$ and inversely proportional to the modulus of elasticity, then, for a same value of K_I, the smaller the value of G_I[11].

Figure 8 presents the results of fracture resistance for concrete of class 25 MPa in the different matrices studied. All the geopolymer small beams presented the plateau of the R_I-curve above the plateau of PCC_25, revealing its superiority in this parameter indicative of the toughness. Among the geopolymer beams, however, the best performance related to resistance to crack propagation was for GCC_25, with values 20% higher than for the GCC-20FA_25 and 50% higher than the GCC-20FA-RHA_25. This corroborates with results obtained in the K_I analysis.

Figure 6. Variation of the rate of deformation energy release with the extension of the crack for concrete notched beams of strength class of 25 MPa with different matrices.

Figure 7 shows the values of G_I as a function of Δa for the notched beams of class 40 MPa and of different matrices.
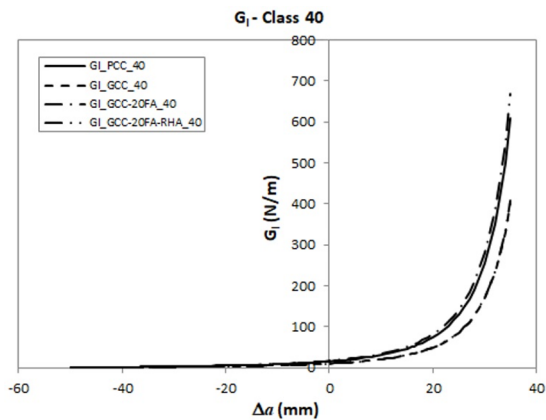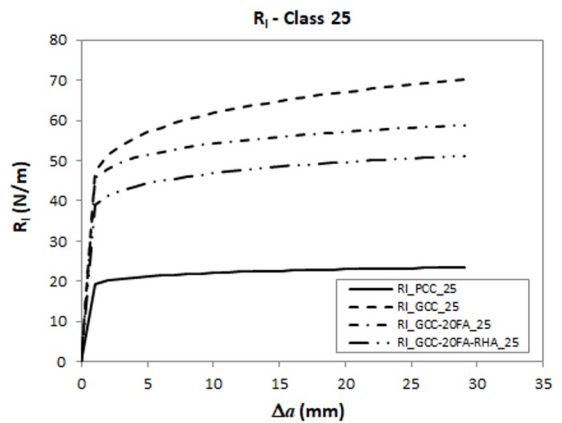

Figure 7. Variation of deformation energy release rate with the extension of the crack for concrete notched beams of strength class of 40 MPa with, different matrices.

G_I curves overlapped for GCC_40 and GCC-20FA-RHA_40 and for PCC_40 and GCC-20FA_40. These results were unexpected since the geopolymers had shown superior or equivalent behavior to PCC_40 in several other parameters as shown above, including K_I.

Figure 8. Variation of the R_I curves with the extension of the crack for concrete notched beams of strength class of 25 MPa, with different matrices.

The results obtained for class 40 MPa were lower than expected. The R_I-curve plateau for GCC_40 has fallen to half the value for GCC_25 (Figure 9).
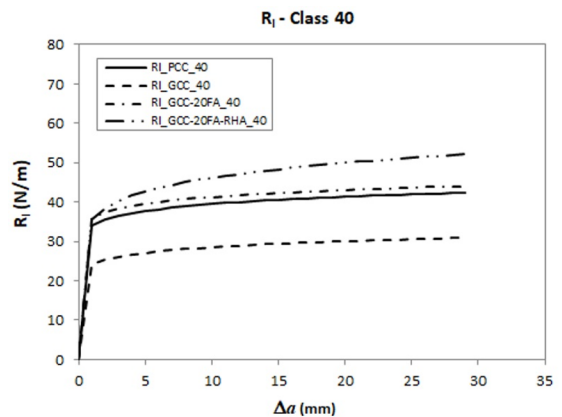

Figure 9. Variation of the R_I curves with the extension of the crack for notched beams of concrete strength class of 40 MPa, with different matrices.

The presence of fly ash and rice husk in the geopolymer did not have a significant influence on the performance of the different strength concrete classes. Whereas the GCC-20FA lost 20% of the resistance to the fracture with the increase of the strength class of the concrete.

Figures 10 and 11 show the average P-δ curves obtained for each type of concrete studied, by classes 25 and 40, respectively.
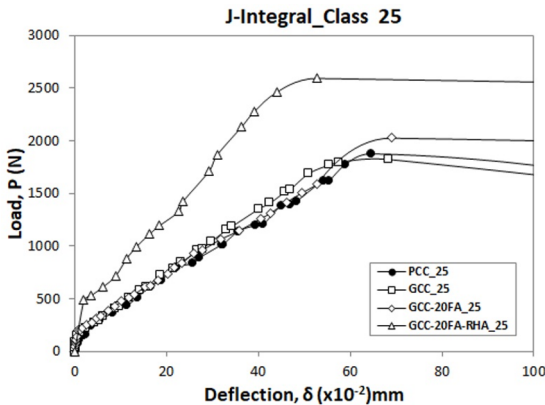

Figure 10. Average values of load-deflection curves in the middle of the span of the class 25 notched beams of different matrices.
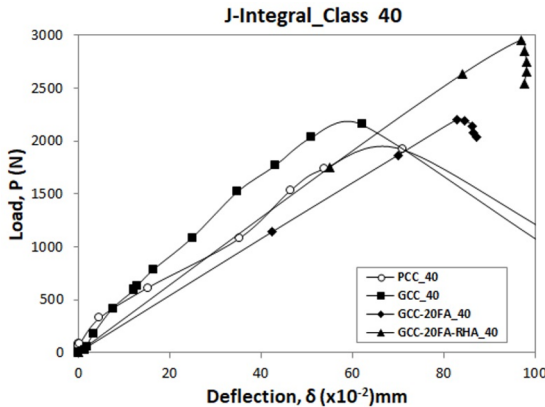

Figure 11. Average values of load-deflection curves in the middle of the span of the class 40 notched beams of different matrices.

Except for PCC notched beams, all the others presented increase of P_{max} with the increase of strength class, especially the GCC-20FA-RHA.

The GCC showed increased stiffness with increased strength class, as expected. However, the other geopolymeric matrices, as well as the PCC, countered this expectation.

Table 2 compares the average values of the critical values of the fracture parameters for the notched beams of the different matrices and strength classes. For the 25 MPa strength class, all geopolymers beams had fracture properties better than PCC_25.

Table 2. Average values of fracture parameters.

Notched Beam	K_{Ic}(MPa. mm$^{1/2}$)	G_{Ic}(N/m)	R_{Ic}(N/m)	*Jmáx*(J/ m^2)
PCC_25	28.45 ± 5.10	22.37 ± 6.59	22.38 ± 6.59	329.76± 55.59
GCC_25	46.08 ± 14.82	68.12 ± 23.31	68.14 ± 23.32	443.14± 151.09
GCC-20FA_25	38.72 ± 3.96	56.03 ± 11.41	56.04 ± 11.41	576.37± 147.01
GCC-20FA-RHA_25	50.17 ± 5.98	44.60 ± 4.55	44.62 ± 4.55	543.90± 135.32
PCC_40	37.01 ± 4.22	40.36 ± 10.73	40.37 ± 10.73	146.93± 12.88
GCC_40	38.60 ± 5.29	29.46 ± 11.92	29.47 ± 11.93	358.15± 93.70
GCC-20FA_40	38.50 ± 2.91	41.91 ± 14.95	41.93 ± 14.96	386.17± 115.76
GCC-20FA-RHA_40	61.18 ± 8.06	50.21 ± 6.46	50.23 ± 6.47	454.15± 56.27

Observing the K_{Ic} parameters, there was loss of toughness of the geopolymer class 25 with the substitution of metakaolin with FA, but there was an increase when the RHA silicate was used. In the notched beams of class 40, the superiority of geopolymer relative to Portland concrete was observed. The fracture toughness, K_{Ic}^{s}, of GCC-20FA-RHA_40 was 65.3%, 58.5% and 58.9% higher than PCC_40, GCC_40 and GCC-20FA_40, respectively. The RHA silicate could simultaneously increase the load bearing capacity and deflection of the beams in both strength classes, showing its potential as an alkali-activator and source of amorphous silica.

4. Conclusions

The analysis of the fracture properties of the concrete notched beams allowed the verification that for the same class of compressive strength, the geopolymer cement concrete is tougher than the Portland equalivant. Replacing the metakaolin with 20% volume fly ash (GCC-20FA) and rice rusk ash based silicate (GCC-20FA-RHA) further improved the performance of the concrete. The fracture toughness of GCC-20FA and GCC-20FA-RHA were measured from parameters such as K_{Ic}, J-Integral and R-curves, and showed values 100% higher than the Portland cement concrete.

5. Acknowledgment

6. References

1. Vargas AS, Dal Molin DCC, Vilela ACF, Silva FJ, Pavão B, Veit H. The effects of Na_2O/SiO_2 molar ratio, curing temperature and age on compressive strength, morphology and microstructure of alkali-activated fly ash-based geopolymers. *Cement & Concrete Composites*. 2011;33(6):653-660.

2. Silva FJ, Barbosa VFF, Thaumaturgo C. Use of Environmental Scanning Microscopy (ESEM) for Study of Alkali-Activated Pulverized Fly Ash. In: *Proceedings of 6th Brazilian Conference on Microscopy of Materials*; 1998 Oct 25-27; Águas de Lindóia, SP, Brazil. 1998. p. 133-136.

3. Barbosa VFF, MacKenzie KJD, Thaumaturgo C. Synthesis and characterization of materials based on inorganic polymers of alumina and sílica: sodium polysialate polymers. *International Journal of Inorganic Materials*. 2000;2(4):309-317.

4. Davidovits J. High-alkali cements for 21st century concretes. In: *Concrete Technology, Past, Present Aand Future, ACI SP-114*. Farmington Hills: American Concrete Institute; 1994. p. 383-398.

5. Xu H, Van Deventer JS. The geopolymerization of alumino-silicate minerals. *International Journal of Mineral Processing*. 2000;59(3):247-266.

6. Xu H, Van Deventer JS. Geopolymerisation of multiple minerals. *Minerals Engineering*. 2000;15(12):1131-1139.

7. Davidovits J. *Geopolymer Chemistry and Applications*. 3rd ed. Saint-Quentin: Institut Géopolymère; 2011.

8. Duxson P, Fernández-Jiménez A, Provis JL, Lukey GC, Palomo A, van Deventer JSJ. Geopolymer technology: the current state of the art. *Journal of Materials Science*. 2007;42(9):2917-2933.

9. Bittencourt TN. *Fraturamento do concreto estrutural: aspectos teóricos, computacionais e experimentais, e suas aplicações*. [Free teaching thesis]. São Paulo: Universidade de São Paulo; 1999.

10. Hillerborg A, Modéer M, Petersson PE. Analysis of crack formation and crack growth in concrete by means of fracture mechanics and finite elements. *Cement and Concrete Research*. 1976;6(6):773-781.

11. Jenq Y, Shah SP. Two Parameter Fracture Model for Concrete. *Journal of Engineering Mechanics*. 1985;111(10):1227-1241.

12. Bazant ZP, Kazemi MT. Determination of fracture energy, process zone length and brittleness number from size effect, with application to rock and concrete. *International Journal of Fracture*. 1990;44(2):111-131.

13. RILEM Committee on Fracture Mechanics of Concrete - Test Methods; Shah SP. Determination of fracture parameters ($K_{Ic}{}^s$ and $CTOD_c$) of plain concrete using three-point bend tests. *Materials and Structures*. 1990;23(6):457-460.

14. Shinde SS, Dhamejani CL. Literature Review on Fracture Toughness and Impact Toughness. *International Journal of Innovations in Engineering Research and Technology*. 2015;2(11)1-5.

15. Irwin GR. Analysis of stress and strains near the end of a crack traversing a plate. *Journal of Applied Mechanics*. 1957;24:361-364.

16. Rice JR. A Path Independent Integral and the Approximate Analysis of Strain Concentration by Notches and Cracks. *Journal of Applied Mechanics*. 1968;35(2):375-386.

17. Janssen M, Zuidema J, Wanhill RJH. *Fracture Mechanics*. 2nd ed. Delft: Delft University Press; 2002. 365 p.

18. Xu S, Reinhardt HW. Crack Extension Resistance and Fracture Properties of Quasi-Brittle Softening Materials like Concrete Based on The Complete Process of Fracture. *International Journal of Fracture*. 1998;92:71-99.

19. Ouyang C, Mobasher B, Shah SP. An R-curve approach for fracture of quasi-britlle materials. *Cement and Concrete Research*. 1990;37(4):901-913.